Original Article
Yonsei Med J 2023 May;64(5):320-326
https://doi.org/10.3349/ymj.2022.0548
Yonsei Medical Journal
YMJ
pISSN: 0513-5796 · eISSN: 1976-2437

# Prediction of Microsatellite Instability in Colorectal Cancer Using a Machine Learning Model Based on PET/CT Radiomics

Soyoung Kim[1], Jae-Hoon Lee[1], Eun Jung Park[2], Hye Sun Lee[3], Seung Hyuk Baik[2], Tae Joo Jeon[1], Kang Young Lee[4], Young Hoon Ryu[1], and Jeonghyun Kang[2]

Departments of [1]Nuclear Medicine and [2]Surgery, Gangnam Severance Hospital, Yonsei University College of Medicine, Seoul; [3]Biostatistics Collaboration Unit, Yonsei University College of Medicine, Seoul; [4]Department of Surgery, Severance Hospital, Yonsei University College of Medicine, Seoul, Korea.

**Purpose:** We investigated the feasibility of preoperative $^{18}$F-fluorodeoxyglucose (FDG) positron emission tomography (PET)/computed tomography (CT) radiomics with machine learning to predict microsatellite instability (MSI) status in colorectal cancer (CRC) patients.

**Materials and Methods:** Altogether, 233 patients with CRC who underwent preoperative FDG PET/CT were enrolled and divided into training (n=139) and test (n=94) sets. A PET-based radiomics signature (rad_score) was established to predict the MSI status in patients with CRC. The predictive ability of the rad_score was evaluated using the area under the receiver operating characteristic curve (AUROC) in the test set. A logistic regression model was used to determine whether the rad_score was an independent predictor of MSI status in CRC. The predictive performance of rad_score was compared with conventional PET parameters.

**Results:** The incidence of MSI-high was 15 (10.8%) and 10 (10.6%) in the training and test sets, respectively. The rad_score was constructed based on the two radiomic features and showed similar AUROC values for predicting MSI status in the training and test sets (0.815 and 0.867, respectively; $p$=0.490). Logistic regression analysis revealed that the rad_score was an independent predictor of MSI status in the training set. The rad_score performed better than metabolic tumor volume when assessed using the AUROC (0.867 vs. 0.794, $p$=0.015).

**Conclusion:** Our predictive model incorporating PET radiomic features successfully identified the MSI status of CRC, and it also showed better performance than the conventional PET image parameters.

**Key Words:** Colorectal cancer, microsatellite instability, positron emission tomography, image analysis, machine learning

## INTRODUCTION

Microsatellites are small, repeating DNA stretches scattered throughout the entire genome.[1] Microsatellite instability (MSI) is a hypermutable phenotype caused by an aberrant DNA repair system related to a high mutation burden.[2] MSI is detected in sporadic cancers of the colon, stomach, and endometrium.[1]

Colorectal cancer (CRC) is the third most common cancer worldwide,[3] and MSI is detected in approximately 15%–20% of CRC.[1] MSI status is important in patients with CRC for pre-

**Received:** December 20, 2022 **Revised:** March 11, 2023 **Accepted:** March 20, 2023 **Published online:** April 20, 2023
**Co-corresponding authors:** Jae-Hoon Lee, MD, PhD, Department of Nuclear Medicine, Gangnam Severance Hospital, Yonsei University College of Medicine, 211 Eonju-ro, Gangnam-gu, Seoul 06273, Korea.
E-mail: docnuke@yuhs.ac and
Jeonghyun Kang, MD, PhD, Department of Surgery, Gangnam Severance Hospital, Yonsei University College of Medicine, 211 Eonju-ro, Gangnam-gu, Seoul 06273, Korea.
E-mail: ravic@naver.com

•The authors have no potential conflicts of interest to disclose.

dicting patient prognosis and selecting the treatment strategy. Patients with stage II CRCs were contraindicated to receive adjuvant chemotherapy in MSI-high status due to the lack of therapeutic benefits.[4] MSI status also has clinical implications in conjunction with immunotherapy, since MSI-high CRCs show high expression of multiple immune checkpoints, including programmed death-1 (PD-1). The U.S. Food and Drug Administration has approved an anti-PD-1 therapy called pembrolizumab for patients with unresectable or metastatic MSI-high or mismatch repair (MMR)-deficient solid tumors, including CRC.[5]

MSI is detected by immunohistochemical (IHC) staining and polymerase chain reaction (PCR) testing of surgical specimens. However, analysis of MMR protein expression through IHC staining is often affected by fixation conditions, resulting in false-negative errors.[6,7] Furthermore, PCR-based testing by amplifying specific microsatellite repeats is complex and expensive.[2] In this context, a non-invasive method reliably predicting MSI status before surgery would be clinically beneficial.

$^{18}$F-fluorodeoxyglucose (FDG) positron emission tomography (PET)/computed tomography (CT) is widely used to evaluate staging, therapeutic response, recurrence, and prognosis in patients with cancer. FDG PET/CT has recently been used to predict the pathology or gene expression in solid tumors, including CRC.[8-11] To our knowledge, only a few studies have investigated the feasibility of using FDG PET/CT to predict MSI status in gastric cancer and CRC.[12-14] A recent study by Li, et al.[13] demonstrated the possibility of predicting MSI status in CRC using a machine learning model integrating the PET/CT radiomic features. However, the prediction model's performance was not compared with that of conventional PET/CT parameters, such as metabolic tumor volume (MTV) or total glycolysis (TLG), nor with clinical variables.

This study sought to develop a machine learning model using radiomics of FDG PET/CT to predict MSI status in patients with CRC and compare its performance with clinical and conventional PET/CT parameters.

## MATERIALS AND METHODS

### Patient cohorts

In this retrospective study, 233 patients were analyzed. All patients underwent preoperative PET/CT within 1 month before surgery and radical operations for CRC between January 2008 and April 2014. The inclusion criteria for this study were the availability of preoperative PET/CT and tests for MSI. The exclusion criteria were patients who 1) underwent preoperative chemoradiotherapy for rectal cancer, 2) underwent emergency operations, and 3) had a history of hereditary nonpolyposis CRC, ulcerative colitis, or Crohn's disease (Supplementary Fig. 1, only online).

The study protocol adhered to the ethical standards of the institutional and national research committees and the 1964 Helsinki Declaration and its later amendments. The Institutional Review Board of the Gangnam Severance Hospital, Yonsei University College of Medicine, approved this study (IRB No. 3-2021-0305) and waived the requirement for written informed consent owing to the retrospective study design.

### PET/CT protocol

All patients fasted for at least 6 hours before PET/CT examination and were confirmed to have blood glucose levels of <180 mg/dL. PET/CT scans were performed 60 min after the intravenous administration of FDG (5.5 MBq/kg of body weight) using a hybrid PET/CT scanner (Biograph 40 TruePoint or Biograph mCT 64, Siemens Healthcare Solutions USA, Inc., Knoxville, TN, USA). A low-dose non-contrast-enhanced CT scan was first obtained for attenuation correction using automatic dose modulation (120 kVp, 40 mAs, and 3-mm slice thickness). PET data were then acquired from the skull base to the proximal thigh for 3 min per bed position in three-dimensional (3D) mode. Images were reconstructed onto a 168×168 matrix using ordered subset expectation maximization with attenuation using two iterations and 21 subsets. The reconstructed images were converted to standardized uptake value (SUV) images as follows: SUV=(decay-corrected activity [kBq] per mL of tissue volume)/(injected FDG activity [kBq] per gram of body mass).

### Radiologic feature extraction

First, a spherical volume of interest (VOI) was manually drawn large enough to include the primary CRC by the two experienced nuclear medicine physicians. Then, manual adjustment was performed to exclude adjacent metastatic lymph nodes and physiologic organ uptake. Contrast-enhanced CT and magnetic resonance imaging, whichever was available, were sometimes used to help delineate the primary CRC. Afterwards, the primary tumor within the VOI was automatically delineated using the contrast-based threshold method implemented in open-source LIFEx software version 7.0.0 (www.lifexsoft.org).[15] The threshold ($T_{CB}$) is defined by: $T_{CB}$=0.5×SUVpeak+SUVbgd, where SUVpeak is a 1 mL spherical region located on the maximum value of the ROI. SUVbgd is defined as the mean uptake in a 3D shell of one-voxel thickness located 2 cm away from the region corresponding to all voxels with a value greater than 70% of the maximum SUV (SUVmax). The original PET data and VOI were saved as medical digital imaging files in the NIfTI format for subsequent radiomic feature extraction. For each patient, 109 quantitative features were extracted from the VOI of the primary tumors on SUV-normalized PET images using the open-source package pyradiomics 3.0.1 (https://github.com/Radiomics/pyradiomics)[16]: 18 first-order statistics, 16 3D shape-based, 24 gray level co-occurrence matrix (GLCM), 16 gray level run length matrix, 16 gray level size zone matrix, 5 neighboring gray tone difference matrix, and 14 gray level dependence matrix textural features. The histogram bin size was fixed at 0.1 SUV; a fixed bin size was used rather than a fixed

number of bins, since tumor SUV ranges differ among patients.[17] A detailed list of parameter adjustments used to extract the tumor area is available at https://pyradiomics.readthedocs.io/en/latest/features.html.

### Determining the MSI status

MSI status was determined from the surgical specimens, as previously described.[18] Briefly, MSI status was identified using five microsatellite markers within the PCR test. MSI-high was diagnosed if the aberrant peaks or peak shifts were observed at two or more microsatellite markers. A case was categorized as MSI low if only one marker showed instability, and as microsatellite stable if no marker had evidence of MSI. MSI-high was identified in 25 (10.7%) patients, and MSI low/microsatellite stable was found in 198 (89.3%) patients.

### Development of rad_score using least absolute shrinkage and selection operator (LASSO) regression and its validation

A total of 233 patients were allocated to the training and test sets using stratified random sampling at a fixed ratio; 60% (n=139) patients were assigned to the training set, and the remaining 40% (n=94) were assigned to the test set. The predictive model, called rad_score, was generated using the least absolute shrinkage and selection operator (LASSO) regression in the training set using PET-derived radiomic features.[19] The LASSO regression model can remove unimportant variables via regression coefficients penalizing the number of parameters. The LASSO regression shrinks the coefficient estimates toward zero, with the degree of shrinkage dependent on an additional parameter λ. Ten-fold cross-validation was used to determine the optimal values for λ using the minimum criteria in our study (Supplementary Fig. 2, only online).

Validation of the rad_score was performed using the area under the receiver operating characteristic curve (AUROC) in the test set. A logistic regression model was used to determine whether the rad_score was an independent predictor of MSI status in CRC. Univariable analysis was performed for the following clinical parameters: sex, age, body mass index (BMI), carcinoembryonic antigen (CEA), tumor location, histologic grade, stage, and the three conventional PET/CT parameters in addition to the rad_score in the training set. The parameters showing statistical significance ($p<0.05$) in the univariable analysis of the training set were subjected to subsequent multivariable analysis in training set with backward stepwise selection. The performance of the rad_score, compared to the three conventional PET parameters (SUVmax, MTV, and TLG), was measured via AUROC analysis.

### Statistical analysis

Clinicopathological characteristics were analyzed using a variance test, where appropriate. The chi-square or Fisher's exact test was used to compare the categorical variables. Continuous variables were analyzed using Student's t-test or the Mann-Whitney U test. Univariable analysis was performed to calculate the odds ratio (OR) of a single variable in the logistic regression model. Univariable analysis denoted the association between MSI-high and the parameter through 1:1 matching. A two-sided $p$-value of less than 0.05 was considered statistically significant. All statistical analyses were performed using R version 3.6.3 (R Foundation for Statistical Computing, Vienna, Austria, https://www.r-project.org).

## RESULTS

### Patient characteristics

The study population comprised 136 male and 97 female. Their age was 64±12 years, and their BMI was 23.2±3.2 kg/m$^2$. The preoperative CEA level was 10.4±28.8 ng/mL. Cancer of the left colon was the most common (44.6%), followed by that of the right colon (34.8%) and the rectum (20.6%). There were no significant differences in clinical and conventional PET/CT parameters between the training and test sets (Table 1). MSI-high was found in 25 of 233 patients (10.7%); the incidence of MSI-high was 10.8% (15/139) in the training set and 10.6% (10/94) in the test set.

### Generation and validation of rad_score

Two radiomic features, original_shape_MinorAxisLength and original_glcm_JointEntropy, with coefficients of 0.06027638 and 0.15312113, respectively, were selected for rad_score. The detailed definition of rad_score is described in Supplementary Fig. 2 (only online).

The rad_score showed good performance in predicting MSI-high status in both the training (AUROC=0.815) and test sets (AUROC=0.867, $p$=0.490) (Fig. 1). The rad_score was determined as an independent predictor of MSI status in CRC when assessed using the logistic regression model with conventional PET/CT and clinical parameters. Univariable analysis of the training set demonstrated that histologic grade, stage, MTV, TLG, and rad_score were significant predictors of MSI status ($p$=0.003, 0.005, 0.001, 0.008, and <0.001, respectively), and CEA was deemed potentially significant ($p$=0.094) (Table 2). Subsequently, these five variables were included in the multivariable logistic regression analysis. After backward stepwise selection, the final predictive model consisted of histologic grade, stage, and rad_score. Multivariable analysis revealed that the rad_score was significantly associated with MSI status in the training set [OR, 1.012 (1.004–1.020); $p$=0.004] (Table 3). The rad_score outperformed SUVmax, MTV, and TLG, when assessed by AUROC (0.590, 0.794, and 0.777, respectively) (Fig. 2).


https://doi.org/10.3349/ymj.2022.0548

**Table 1.** Comparison of Clinical and Conventional PET/CT Parameters between Training and Test Sets

| | Training set (n=139) | Test set (n=94) | *p* |
|---|---|---|---|
| Sex | | | 0.658 |
| Female | 60 (43.2) | 37 (39.4) | |
| Male | 79 (56.8) | 57 (60.6) | |
| Age (yr) | | | 0.620 |
| <70 | 83 (59.7) | 60 (63.8) | |
| ≥70 | 56 (40.3) | 34 (36.2) | |
| BMI (kg/m$^2$) | | | 0.565 |
| <25 | 99 (71.2) | 71 (75.5) | |
| ≥25 | 40 (28.8) | 23 (24.5) | |
| CEA (ng/mL) | | | 0.692 |
| <5 | 92 (66.2) | 59 (62.8) | |
| ≥5 | 47 (33.8) | 35 (37.2) | |
| Tumor location | | | 0.688 |
| Right colon | 51 (36.7) | 30 (31.9) | |
| Left colon | 59 (42.4) | 45 (47.9) | |
| Rectum | 29 (20.9) | 19 (20.2) | |
| Histologic grade | | | 0.246 |
| G1 & G2 | 130 (93.5) | 83 (88.3) | |
| G3 & MC & SRC | 9 (6.5) | 11 (11.7) | |
| Stage | | | >0.999 |
| I & II | 66 (47.5) | 45 (47.9) | |
| III & IV | 73 (52.5) | 49 (52.1) | |
| MSI | | | >0.999 |
| MSI-high | 15 (10.8) | 10 (10.6) | |
| SUVmax | | | 0.986 |
| Continuous variable | 13.0±6.5 | 13.0±6.1 | |
| MTV | | | 0.100 |
| Continuous variable | 21.6±19.0 | 26.5±24.1 | |
| TLG | | | 0.140 |
| Continuous variable | 166.7±194.3 | 207.4±221.2 | |
| Rad_score | | | 0.058 |
| Continuous variable | 107.9±80.5 | 131.6±100.3 | |

BMI, body mass index; CEA, carcinoembryonic antigen; MC, mucinous adenocarcinoma; SRC, signet-ring cell; MSI, microsatellite instability; SUVmax, maximum standardized uptake value; MTV, metabolic tumor volume; TLG, total lesion glycolysis.
Data are presented as mean±standard deviation or n (%).

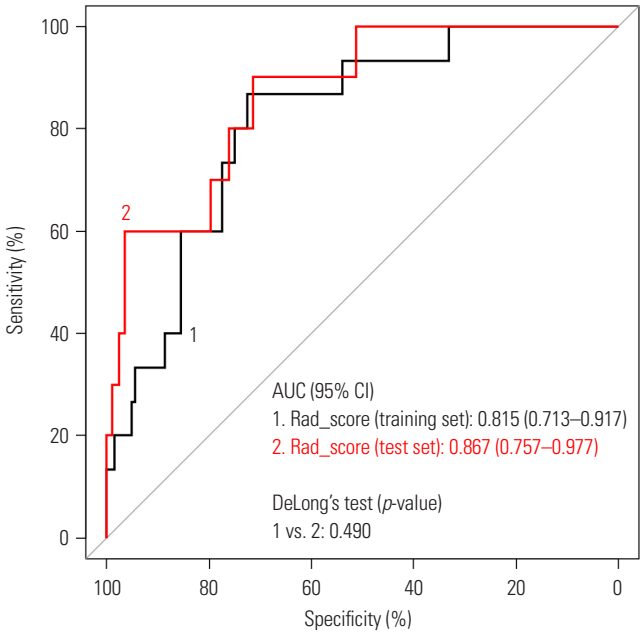


**Fig. 1.** Comparison of AUC of LASSO-derived rad_score in the training and test sets. AUC, area under the curve; LASSO, least absolute shrinkage and selection operator; CI, confidence interval.

## DISCUSSION

Our study demonstrated that radiomics feature-derived preoperative FDG PET/CT images could predict MSI status with a high predictive value of 0.867 AUROC. This predictability outperforms conventional PET-derived parameters in patients with CRC, such as SUVmax, MTV, and TLG. Univariable and multivariable analyses revealed that the rad_score was a significant predictor of MSI status in CRC.

MSI status is associated with patient prognosis, and its pivotal predictive role is to offer adjuvant chemotherapy, especially in patients with stage II colon cancer.[20,21] Immunotherapy may depend on the MSI status; thus, this biomarker is one of the most powerful indicators of immunotherapy response in various cancers. Currently, MSI status can be assessed using specimens obtained from biopsies or surgeries using IHC or PCR tests. IHC is inexpensive but is affected by the fixation of tissue samples and neoadjuvant chemoradiation, and PCR is complex and expensive.[2,6,7] Therefore, several investigators have suggested deep learning-based MSI prediction algorithms using whole-slide images.[22-25] Nevertheless, a whole-slide image after surgery is usually required in these deep-learning-based MSI predictions, such that it can be applied to patients who have undergone surgery. Nevertheless, research using CT or PET to predict MSI is of increasing interest, as it is non-invasive and has the advantage of being applied to patients who cannot undergo surgery.

Radiomics provides valuable information that may be invisible to the naked human eye by extracting multiple features from medical images.[26] Radiomics may reflect tumor biology in human tissues at the cellular and genetic levels.[27,28] PET-based radiomics studies have recently been developed for preoperative pathology prediction and survival in many cancers.[29] In CRC, several studies have reported that radiomic analysis of features of PET/CT images could predict regional lymph node metastasis, perineural invasion, genetic alteration, treatment response, and prognosis.[30-33] Although MSI status is critical for choosing a treatment strategy and predicting prognosis in patients with CRC, only a few data are available on the ability of radiomics to predict MSI status in CRC. While two previous studies showed fair/good predictive performance of CT-based

**Table 2.** Univariable Analysis Associated with the MSI Status in Training Set

| | OR (95% CI) | *p* |
|---|---|---|
| Sex | | |
| Female | Ref | |
| Male | 0.631 (0.209–1.866) | 0.402 |
| Age (yr) | | |
| <70 | Ref | |
| ≥70 | 0.715 (0.212–2.141) | 0.562 |
| BMI (kg/m$^2$) | | |
| <25 | Ref | |
| ≥25 | 0.587 (0.128–1.981) | 0.431 |
| CEA (ng/mL) | | |
| <5 | Ref | |
| ≥5 | 0.270 (0.041–1.035) | 0.094 |
| Tumor location | | |
| Right colon | Ref | |
| Left colon | 0.298 (0.077–0.960) | 0.053 |
| Rectum | 0.146 (0.007–0.829) | 0.074 |
| Histologic grade | | |
| G1 & G2 | Ref | |
| G3 & MC & SRC | 8.654 (1.911–37.691) | 0.003 |
| Stage | | |
| I & II | Ref | |
| III & IV | 0.114 (0.017–0.438) | 0.005 |
| SUVmax | | |
| Continuous variable* | 1.039 (0.956–1.111) | 0.342 |
| MTV | | |
| Continuous variable* | 1.038 (1.015–1.065) | 0.001 |
| TLG | | |
| Continuous variable* | 1.003 (1.001–1.006) | 0.008 |
| Rad_score | | |
| Continuous variable* | 1.010 (1.005–1.017) | <0.001 |

MSI, microsatellite instability; OR, odds ratio; CI, confidence interval; BMI, body mass index; CEA, carcinoembryonic antigen; MC, mucinous adenocarcinoma; SRC, signet-ring cell; SUVmax, maximum standardized uptake value; MTV, metabolic tumor volume; TLG, total lesion glycolysis.
*Per 1 unit.

**Table 3.** Multivariable Analysis Associated with the MSI in Training Set

| | OR (95% CI) | *p* |
|---|---|---|
| Histologic grade | | |
| G1 & G2 | Ref | |
| G3 & MC & SRC | 14.573 (1.972–107.697) | 0.009 |
| Stage | | |
| I & II | Ref | |
| III & IV | 0.085 (0.014–0.503) | 0.007 |
| Rad_score | | |
| Continuous variable (Per 1 unit) | 1.012 (1.004–1.020) | 0.004 |

MSI, microsatellite instability; OR, odds ratio; CI, confidence interval; MC, mucinous adenocarcinoma; SRC, signet-ring cell.

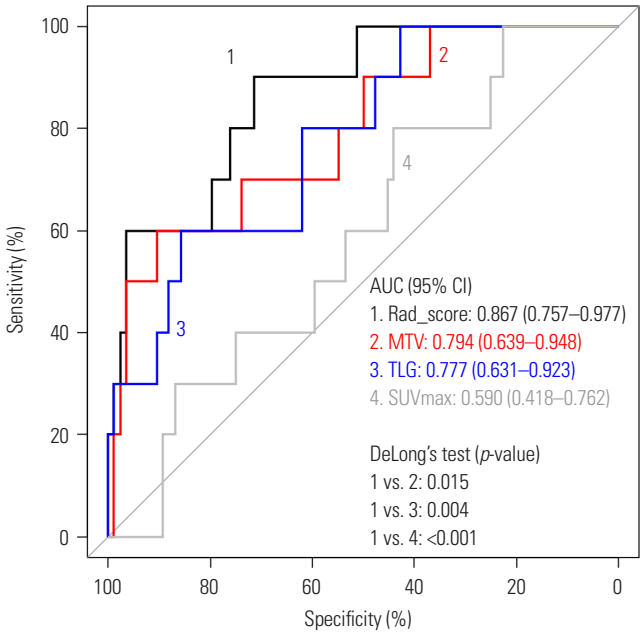


**Fig. 2.** Comparison of AUC between rad_score and conventional PET parameters in the test set. AUC, area under the curve; CI, confidence interval; MTV, metabolic tumor volume; TLG, total lesion glycolysis; SUVmax, maximum standardized uptake value; PET, positron emission tomography.

radiomic features with AUCs of 0.765–0.792,[34,35] PET/CT could provide additional functional information. Chung, et al.[12] reported that the median SUVmax in patients with MSI-high was higher than that of microsatellite-stable patients in 131 patients with gastric cancer, showing the possibility of using PET images to evaluate molecular deterioration in patients with cancer. To our knowledge, only one study has investigated the association between PET/CT-derived radiomic features and MSI status in CRC patients. Li, et al.[13] suggested a model using the balanced bagging algorithm, showing an AUC of 0.828. Notably, in the current study, we achieved a higher AUC (0.867) to predict MSI status than in the previous study. Furthermore, we performed logistic regression analysis and showed that the rad_score significantly predicted MSI status in CRC.

Histologic features that predict MSI status are tumor-infiltrating lymphocytes, Crohn's-like lymphoid reaction, mucinous/signet ring differentiation, and medullary growth pattern.[36] Two radiomic features incorporated in the rad_score are the joint entropy of the GLCM features and the minor axis length of the shape features. GLCM joint entropy is defined as a measurement of the variability of the neighborhood strength value and shapes minor axis length as the length of the second-largest axis of the ROI.[37] Interestingly, Hotta, et al.[38] reported that GLCM entropy was the most important prognostic PET feature for overall survival and progression-free survival in rectal cancer patients. While there is no correlation between GLCM entropy and histologic features of MSI-high CRC, one study reported that GLCM entropy was associated with the density of tumor-infiltrating lymphocytes in hepatocellular carcinoma.[39]


https://doi.org/10.3349/ymj.2022.0548

In this context, we suppose that joint entropy, as one of the GLCM entropies, could be associated with tumor-infiltrating lymphocytes in MSI-high CRC and was therefore found to be a strong predictor in this study. Although the shape features are relatively simpler than the other higher-order radiomic features, no data is available for MSI-high solid tumors. Hypothetically, the heterogeneous components of mucin accumulation in MSI-high tumors may result in a significant difference in the shape features of MSI-low or microsatellite stable tumors; however, further studies are needed to elucidate the association between the minor axis length of the shape and MSI-high tumors.

Our study had several limitations. This study was retrospective and performed at a single institution without external validation, limiting our results' generalizability. Although internal validation was carried out, external validation in a multicenter study is required. More importantly, to enroll more MSI-high cases, we combined the studies from different PET/CT scanners, which could affect the robustness of the extracted radiomic features in this study. While this study demonstrated the feasibility of machine learning using PET/CT radiomics to predict the MSI status in CRC, our results need to be interpreted as explorative and investigated under the various acquisition and reconstruction methods. In addition, the absence of a standardized method for tumor segmentation in PET radiomics analysis can be an obstacle to generalizing the study results because the radiomic feature selection and model performance can vary according to the lesion segmentation methods.[40,41]

This study used a machine learning algorithm and PET radiomic features to construct a prediction model to determine the MSI status in CRC. Our radiomics model could successfully predict the MSI status of CRC, and showed better predictive performance than conventional PET imaging parameters.

## AUTHOR CONTRIBUTIONS

Conceptualization: Jae-Hoon Lee and Jeonghyun Kang. Data curation: Eun Jung Park, Seung Hyuk Baik, Soyoung Kim, and Tae Joo Jeon. Formal analysis: Hye Sun Lee, Jeonghyun Kang, Soyoung Kim, Jae-Hoon Lee, and Tae Joo Jeon. Investigation: Tae Joo Jeon, Kang Young Lee, Eun Jung Park, Jeonghyun Kang, and Jae-Hoon Lee. Methodology: Soyoung Kim, Jae-Hoon Lee, Hye Sun Lee, and Tae Joo Jeon. Project administration: Jae-Hoon Lee, Young Hoon Ryu, and Jeonghyun Kang. Resources: Seung Hyuk Baik, Kang Young Lee, and Eun Jung Park. Software: Hye Sun Lee and Jeonghyun Kang. Supervision: Young Hoon Ryu, Seung Hyuk Baik, and Kang Young Lee. Validation: Tae Joo Jeon, Seung Hyuk Baik, and Kang Young Lee. Visualization: Hye Sun Lee. Writing—original draft: Soyoung Kim and Jae-Hoon Lee. Writing—review & editing: Kang Young Lee, Young Hoon Ryu, and Jeonghyun Kang. Approval of final manuscript: all authors.

## ORCID iDs

Soyoung Kim https://orcid.org/0000-0002-6163-1434
Jae-Hoon Lee https://orcid.org/0000-0002-9898-9886
Eun Jung Park https://orcid.org/0000-0002-4559-2690
Hye Sun Lee https://orcid.org/0000-0001-6328-6948
Seung Hyuk Baik https://orcid.org/0000-0003-4183-2332
Tae Joo Jeon https://orcid.org/0000-0002-7574-6734
Kang Young Lee https://orcid.org/0000-0001-5944-2063
Young Hoon Ryu https://orcid.org/0000-0002-9000-5563
Jeonghyun Kang https://orcid.org/0000-0001-7311-6053

## REFERENCES

1. Nojadeh JN, Behrouz Sharif S, Sakhinia E. Microsatellite instability in colorectal cancer. EXCLI J 2018;17:159-68.
2. Boland CR, Goel A. Microsatellite instability in colorectal cancer. Gastroenterology 2010;138:2073-87.e3.
3. Bray F, Ferlay J, Soerjomataram I, Siegel RL, Torre LA, Jemal A. Global cancer statistics 2018: GLOBOCAN estimates of incidence and mortality worldwide for 36 cancers in 185 countries. CA Cancer J Clin 2018;68:394-424.
4. Jover R, Zapater P, Castells A, Llor X, Andreu M, Cubiella J, et al. The efficacy of adjuvant chemotherapy with 5-fluorouracil in colorectal cancer depends on the mismatch repair status. Eur J Cancer 2009;45:365-73.
5. Lemery S, Keegan P, Pazdur R. First FDA approval agnostic of cancer site - when a biomarker defines the indication. N Engl J Med 2017;377:1409-12.
6. Kawakami H, Zaanan A, Sinicrope FA. Microsatellite instability testing and its role in the management of colorectal cancer. Curr Treat Options Oncol 2015;16:30.
7. Chen W, Swanson BJ, Frankel WL. Molecular genetics of microsatellite-unstable colorectal cancer for pathologists. Diagn Pathol 2017;12:24.
8. Kawada K, Toda K, Nakamoto Y, Iwamoto M, Hatano E, Chen F, et al. Relationship between 18F-FDG PET/CT scans and KRAS mutations in metastatic colorectal cancer. J Nucl Med 2015;56:1322-7.
9. Li Y, Zhang Y, Fang Q, Zhang X, Hou P, Wu H, et al. Radiomics analysis of [18F]FDG PET/CT for microvascular invasion and prognosis prediction in very-early- and early-stage hepatocellular carcinoma. Eur J Nucl Med Mol Imaging 2021;48:2599-614.
10. Nagarajah J, Ho AL, Tuttle RM, Weber WA, Grewal RK. Correlation of BRAFV600E mutation and glucose metabolism in thyroid cancer patients: an 18F-FDG PET study. J Nucl Med 2015;56:662-7.
11. Zhang J, Zhao X, Zhao Y, Zhang J, Zhang Z, Wang J, et al. Value of pre-therapy 18F-FDG PET/CT radiomics in predicting EGFR mutation status in patients with non-small cell lung cancer. Eur J Nucl Med Mol Imaging 2020;47:1137-46.
12. Chung HW, Lee SY, Han HS, Park HS, Yang JH, Lee HH, et al. Gastric cancers with microsatellite instability exhibit high fluorodeoxyglucose uptake on positron emission tomography. Gastric Cancer 2013;16:185-92.
13. Li J, Yang Z, Xin B, Hao Y, Wang L, Song S, et al. Quantitative prediction of microsatellite instability in colorectal cancer with preoperative PET/CT-based radiomics. Front Oncol 2021;11:702055.
14. Liu H, Ye Z, Yang T, Xie H, Duan T, Li M, et al. Predictive value of metabolic parameters derived from 18F-FDG PET/CT for microsatellite instability in patients with colorectal carcinoma. Front Immunol 2021;12:724464.
15. Nioche C, Orlhac F, Boughdad S, Reuzé S, Goya-Outi J, Robert C, et al. LIFEx: a freeware for radiomic feature calculation in multimodality imaging to accelerate advances in the characterization of tumor heterogeneity. Cancer Res 2018;78:4786-9.
16. van Griethuysen JJM, Fedorov A, Parmar C, Hosny A, Aucoin N, Narayan V, et al. Computational radiomics system to decode the radiographic phenotype. Cancer Res 2017;77:e104-7.

17. Leijenaar RT, Nalbantov G, Carvalho S, van Elmpt WJ, Troost EG, Boellaard R, et al. The effect of SUV discretization in quantitative FDG-PET radiomics: the need for standardized methodology in tumor texture analysis. Sci Rep 2015;5:11075.
18. Kang J, Lee HW, Kim IK, Kim NK, Sohn SK, Lee KY. Clinical implications of microsatellite instability in T1 colorectal cancer. Yonsei Med J 2015;56:175-81.
19. Chang C, Sun X, Wang G, Yu H, Zhao W, Ge Y, et al. A machine learning model based on PET/CT radiomics and clinical characteristics predicts ALK rearrangement status in lung adenocarcinoma. Front Oncol 2021;11:603882.
20. Ribic CM, Sargent DJ, Moore MJ, Thibodeau SN, French AJ, Goldberg RM, et al. Tumor microsatellite-instability status as a predictor of benefit from fluorouracil-based adjuvant chemotherapy for colon cancer. N Engl J Med 2003;349:247-57.
21. Watanabe T, Wu TT, Catalano PJ, Ueki T, Satriano R, Haller DG, et al. Molecular predictors of survival after adjuvant chemotherapy for colon cancer. N Engl J Med 2001;344:1196-206.
22. Yamashita R, Long J, Longacre T, Peng L, Berry G, Martin B, et al. Deep learning model for the prediction of microsatellite instability in colorectal cancer: a diagnostic study. Lancet Oncol 2021;22:132-41.
23. Lee SH, Song IH, Jang HJ. Feasibility of deep learning-based fully automated classification of microsatellite instability in tissue slides of colorectal cancer. Int J Cancer 2021;149:728-40.
24. Echle A, Grabsch HI, Quirke P, van den Brandt PA, West NP, Hutchins GGA, et al. Clinical-grade detection of microsatellite instability in colorectal tumors by deep learning. Gastroenterology 2020;159:1406-16.e11.
25. Kather JN, Pearson AT, Halama N, Jäger D, Krause J, Loosen SH, et al. Deep learning can predict microsatellite instability directly from histology in gastrointestinal cancer. Nat Med 2019;25:1054-6.
26. Cook GJR, Goh V. A role for FDG PET radiomics in personalized medicine? Semin Nucl Med 2020;50:532-40.
27. Aerts HJ, Velazquez ER, Leijenaar RT, Parmar C, Grossmann P, Carvalho S, et al. Decoding tumour phenotype by noninvasive imaging using a quantitative radiomics approach. Nat Commun 2014;5:4006.
28. Jiang Y, Yuan Q, Lv W, Xi S, Huang W, Sun Z, et al. Radiomic signature of 18F fluorodeoxyglucose PET/CT for prediction of gastric cancer survival and chemotherapeutic benefits. Theranostics 2018;8:5915-28.
29. Lee JW, Lee SM. Radiomics in oncological PET/CT: clinical applications. Nucl Med Mol Imaging 2018;52:170-89.
30. Chen SW, Shen WC, Chen WT, Hsieh TC, Yen KY, Chang JG, et al. Metabolic imaging phenotype using radiomics of [18F]FDG PET/CT associated with genetic alterations of colorectal cancer. Mol Imaging Biol 2019;21:183-90.
31. He J, Wang Q, Zhang Y, Wu H, Zhou Y, Zhao S. Preoperative prediction of regional lymph node metastasis of colorectal cancer based on 18F-FDG PET/CT and machine learning. Ann Nucl Med 2021;35:617-27.
32. Ma J, Guo D, Miao W, Wang Y, Yan L, Wu F, et al. The value of 18F-FDG PET/CT-based radiomics in predicting perineural invasion and outcome in non-metastatic colorectal cancer. Abdom Radiol (NY) 2022;47:1244-54.
33. Kang J, Lee JH, Lee HS, Cho ES, Park EJ, Baik SH, et al. Radiomics features of 18F-fluorodeoxyglucose positron-emission tomography as a novel prognostic signature in colorectal cancer. Cancers (Basel) 2021;13:392.
34. Fan S, Li X, Cui X, Zheng L, Ren X, Ma W, et al. Computed tomography-based radiomic features could potentially predict microsatellite instability status in stage II colorectal cancer: a preliminary study. Acad Radiol 2019;26:1633-40.
35. Golia Pernicka JS, Gagniere J, Chakraborty J, Yamashita R, Nardo L, Creasy JM, et al. Radiomics-based prediction of microsatellite instability in colorectal cancer at initial computed tomography evaluation. Abdom Radiol (NY) 2019;44:3755-63.
36. Hildebrand LA, Pierce CJ, Dennis M, Paracha M, Maoz A. Artificial intelligence for histology-based detection of microsatellite instability and prediction of response to immunotherapy in colorectal cancer. Cancers (Basel) 2021;13:391.
37. Zwanenburg A, Leger S, Vallières M, Löck S. Image biomarker standardisation initiative. arXiv [Preprint]. 2016 [cited 2022 September 17]. Available at: https://doi.org/10.48550/arXiv.1612.07003.
38. Hotta M, Minamimoto R, Gohda Y, Miwa K, Otani K, Kiyomatsu T, et al. Prognostic value of 18F-FDG PET/CT with texture analysis in patients with rectal cancer treated by surgery. Ann Nucl Med 2021;35:843-52.
39. Liao H, Zhang Z, Chen J, Liao M, Xu L, Wu Z, et al. Preoperative radiomic approach to evaluate tumor-infiltrating CD8+ T cells in hepatocellular carcinoma patients using contrast-enhanced computed tomography. Ann Surg Oncol 2019;26:4537-47.
40. Im HJ, Bradshaw T, Solaiyappan M, Cho SY. Current methods to define metabolic tumor volume in positron emission tomography: which one is better? Nucl Med Mol Imaging 2018;52:5-15.
41. Jun S, Park JG, Seo Y. Accurate FDG PET tumor segmentation using the peritumoral halo layer method: a study in patients with esophageal squamous cell carcinoma. Cancer Imaging 2018;18:35.


https://doi.org/10.3349/ymj.2022.0548